0013-7227/07/$15.00/0
Printed in U.S.A.

Endocrinology 148(2):693–704
Copyright © 2007 by The Endocrine Society
doi: 10.1210/en.2006-0681

Pre-B-Cell Transcription Factor 1 and Steroidogenic Factor 1 Synergistically Regulate Adrenocortical Growth and Steroidogenesis

Urs D. Lichtenauer, Marlena Duchniewicz, Mateusz Kolanczyk, Andreas Hoeflich, Stephanie Hahner, Tobias Else, Andrew B. Bicknell, Tomasz Zemojtel, Nancy R. Stallings, Dominik M. Schulte, Mark P. Kamps, Gary D. Hammer, Jürgen S. Scheele, and Felix Beuschlein

Department of Internal Medicine II (U.D.L., M.D., D.M.S., F.B.), Division of Endocrinology and Metabolism; Department of Internal Medicine I and Center for Clinical Trials (M.D., M.K., T.Z., J.S.S.); and Department of Pharmacology I (J.S.S.), Albert-Ludwigs-University Freiburg, D-79104 Freiburg, Germany; Research Institute for the Biology of Farm Animals (A.H.), Research Unit Genetics and Biometry, D-18196 Dummerstorf, Germany; Department of Internal Medicine (S.H.), Endocrine and Diabetes Unit, University of Wuerzburg, D-97074 Wuerzburg, Germany; Division of Metabolism, Endocrinology, and Diabetes (T.E., G.D.H.), Department of Internal Medicine, University of Michigan, Ann Arbor, Michigan 48109; School of Animal and Microbial Sciences (A.B.B.), University of Reading, Reading RG6 6AH, United Kingdom; Division of Endocrinology and Metabolism (N.R.S.), Department of Internal Medicine, University of Texas Southwestern Medical Center, Dallas, Texas 75390; Department of Pathology (M.P.K.), University of California San Diego, School of Medicine, La Jolla, California 92093; and Division of Endocrine Research (F.B.), Department of Medicine Innenstadt, Ludwig-Maximilians-University, D-80336 Munich, Germany

A variety of transcription factors including Wilms tumor gene (Wt-1), steroidogenic factor 1 (Sf-1), dosage-sensitive sex reversal, adrenal hypoplasia congenita on the X-chromosome, Gene 1 (Dax-1), and pre-B-cell transcription factor 1 (Pbx1) have been defined as necessary for regular adrenocortical development. However, the role of Pbx1 for adrenal growth and function in the adult organism together with the molecular relationship between Pbx1 and these other transcription factors have not been characterized. We demonstrate that Pbx haploinsufficiency ($Pbx1^{+/-}$) in mice is accompanied by a significant lower adrenal weight in adult animals compared with wild-type controls. Accordingly, baseline proliferating cell nuclear antigen levels are lower in $Pbx1^{+/-}$ mice, and unilateral adrenalectomy results in impaired contralateral compensatory adrenal growth, indicating a lower proliferative potential in the context of Pbx1 haploinsufficiency. In accordance with the key role of IGFs in adrenocortical proliferation and development, real-time RT-PCR demonstrates significant lower expression levels of the IGF-I receptor, and up-regulation of IGF binding protein-2. Functionally, $Pbx1^{+/-}$ mice display a blunted corticosterone response after ACTH stimulation coincident with lower adrenal expression of the ACTH receptor (melanocortin 2 receptor, Mc2-r). Mechanistically, *in vitro* studies reveal that Pbx1 and Sf-1 synergistically stimulates Mc2-r promoter activity. Moreover, Sf-1 directly activates the Pbx1 promoter activity *in vitro* and *in vivo*. Taken together, these studies provide evidence for a role of Pbx1 in the maintenance of a functional adrenal cortex mediated by synergistic actions of Pbx1 and Sf-1 in the transcriptional regulation of the critical effector of adrenocortical differentiation, the ACTH receptor. (*Endocrinology* 148: 693–704, 2007)

THE TRANSCRIPTION FACTOR Pbx1 (pre-B-cell transcription factor 1) belongs to the group of non-Hox-homeodomain transcription factors that significantly contribute to embryonic differentiation and organogenesis. During this process, Pbx1 allows homeodomain proteins such as Hox (1), engrailed (2), MyoD (3), Meis (4), or Pdx (5) to bind to DNA with higher affinity and specificity. Complexes of Pbx1/Hox can act as transcriptional activators or as repressors depending on the recruitment of other transcription factors and modulation through extracellular signals. Moreover, Meis and Prep proteins regulate Hox activity both as components of the DNA-bound Hox complex and by regulating Pbx activity in the absence of DNA (6). In addition, recent evidence suggests that Pbx1/Meis dimers penetrate repressive chromatin enabling consecutive binding of cofactors such as Hox or MyoD that in turn results in gene activation or its repression (3). The physiological importance of Pbx1 during development is strongly supported by the intrauterine death of $Pbx1^{-/-}$ mice at embryonic d 15–16 with severe perturbation in organ development (7). These pleiotropic defects associated with Pbx1 deficiency concerns hematopoiesis in the fetal liver (7), pancreas development (8), nephrogenesis (9), and skeleton development (10). As expected from the functional interaction between Pbx1 and Hox proteins, these developmental abnormalities to a great extent overlap phenotypes found in different Hox null mutant mice (11–13).

The significance of Pbx1 for steroidogenesis has been established by earlier studies on Pbx1-dependent expression of

First Published Online November 2, 2006

Abbreviations: Cyp17, 17α-Hydroxylase/17,20-lyase; ES, embryonic stem; 20αhsd, 20α-hydroxysteroid dehydrogenase; IGFBP, IGF-binding protein; Mc2-r, melanocortin 2 receptor; Pbx1, pre-B-cell transcription factor 1; Pcna, proliferating cell nuclear antigen; SF-1, steroidogenic factor 1.

***Endocrinology* is published monthly by The Endocrine Society (http://www.endo-society.org), the foremost professional society serving the endocrine community.**

Downloaded from endo.endojournals.org by on February 21, 2008

17α-hydroxylase/17,20-lyase (Cyp17) (14). Cyp17 is required for cortisol and androgen biosynthesis and therefore plays a key role in biological processes including sexual differentiation. Overexpression of Pbx1 has been demonstrated to enhance the cAMP evoked transcriptional response in an *in vitro* model, thus indicating a modulation of cAMP-dependent transcription through Pbx1. Additional evidence for Pbx1-dependent effects on adrenal function comes from the phenotypical description of significant adrenal and urogenital differentiation defects including severe adrenal hypoplasia (15) in Pbx1$^{-/-}$ animals associated with minimal expression of steroidogenic factor 1 (Sf-1), an important regulator of adrenocortical cell commitment and steroidogenesis. In accordance with this observation, only recently, Pbx1-dependent initiation of Sf-1 expression during murine adrenal development has been demonstrated in a series of transgenic approaches *in vivo* (16).

Taken together, Pbx1 has been implicated as an additional key factor for adrenocortical organogenesis and growth. However, the lethal phenotype of Pbx1$^{-/-}$ animals has precluded the elucidation of possible Pbx1-dependent effects on adrenal function in the adult organism. Therefore, we used a viable, haploinsufficient mouse model lacking the critical domain for Pbx1-DNA interaction to further define the contribution of Pbx1 for adrenal growth and steroidogenesis.

Materials and Methods

Generation of Pbx1 haploinsufficient animals

The Pbx1flox1 targeting vector was constructed by cloning of three adjacent Pbx1 genomic fragments into a pflox plasmid (17) (Fig. 1A). The targeted sequence (referred to as target) was composed of Pbx1 exon 6 (corresponding to 1192–1356 bp in PBX1a mRNA, accession no. AF020196) flanked by 700-bp upstream and 280-bp downstream intronic sequences (Fig. 1A). In the course of Pbx1flox1 vector preparation, a *Hin*dIII restriction digest site was removed from the genomic sequence upstream of the targeted exon 6 (Fig. 1A). Removal of this restriction site by enzymatic digest and Klenow polymerase fill-in reaction allowed for Southern detection of homologous recombination events with the external Southern probe located upstream of the vector sequences (Fig. 1, A and B).

The *Not*I linearized Pbx1flox1 plasmid was electroporated into the embryonic d 14 embryonic stem (ES) cells followed by 6 d of G418 selection. After positive selection with G418, homologous recombinant clones were identified by Southern blot analysis using *Hin*dIII digest and the 5′ external Southern blot probe. This probe hybridized to the 8-kb fragment of the wild-type allele and the 16-kb fragment of a correctly targeted allele (Fig. 1B). The homologous recombination events, detected by Southern blot, were confirmed by PCR amplification of the 5′ and 3′ ends of the targeting vector, with one primer based on the sequence inside and one external to the vector sequence (Fig. 1C). Cells were electroporated with 20 μg CMV-Cre plasmid (kindly provided by Dr. Florian Otto) and serially diluted before plating. Colonies were picked and PCR analyzed for the loss of target and selection cassette sequences (data not shown). Four clones of ES cells heterozygous for the Pbx1 knockout were microinjected into blastocysts of C57BL/6 background. A total of 57 microinjected blastocysts were retransferred into pseudopregnant foster mice, and three highly chimeric males were born. One of the male chimeras gave a germline transmission of the Pbx1 knockout allele that was further bred onto the C57BL/6 background. Genotyping was performed by genomic PCR of tail DNA using primers flanking the targeted exon 6 yielding a 600-bp fragment for the knockout allele and a 1.2-kb fragment for the wild-type allele. Because this long fragment was not regularly amplified under the applied PCR conditions, 18s primers resulting in a 151-bp fragment were used as a positive amplification control (Fig. 1D).

Timed pregnancies of Pbx1 heterozygote F2 generation mice were set up and d-14.5 embryos obtained. Phenotypically Pbx1$^{-/-}$ embryos were similar to Pbx1$^{-/-}$ mice described previously (10). Among externally visible knockout features, Pbx1$^{-/-}$ pups were distinguished by sc edema, diminished vascularization and consequent pallor, slender thorax and abdomen, hunched posture, and abnormal orientation of both fore and hind limbs (data not shown).

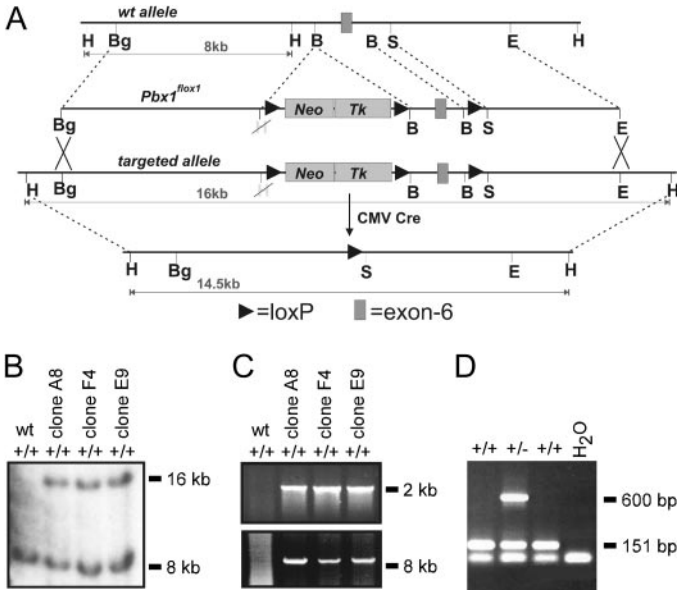

FIG. 1. Schematic representation of the Pbx1 locus and targeting vector. A, Schematic representation of allele targeting by homologous recombination and subsequent transient Cre recombinase expression. As a result of homologous recombination and subsequent Cre expression, sequences containing exon 6 as well as the selection cassette were removed, yielding neomycin (Neo)-sensitive ΔPbx1$^{+/-}$ ES cell clones. B, Southern blot analysis of *Hin*dIII-digested DNA from Pbx1 clones after first homologous recombination before Cre treatment indicated a shift of the wild-type (wt) 8-kb band to 16 kb due to the loss of a *Hin*dIII site in the homology arm. C, Southern blot analysis was confirmed by long-range PCR with primers within and outside of the targeted sequence yielding 8- and 2-kb fragments of the 5′ and 3′ homology arms of the vector. D, Genotyping of wild-type (+/+) and heterozygous Pbx1 knockout animals (+/−) was performed by PCR (see text for details). B, *Bam*HI; Bg, *Bgl*II; E, *Eco*RI; H, *Hin*dIII; N, *Not*I; S, *Sal*I.

Animal experiments

All experiments involving animals were performed in accordance with institutionally approved and current animal care guidelines. Animals were maintained under standard conditions of temperature (22 C) and lighting (12 h light, 12 h dark) and with food and water given *ad libitum*. Pbx1$^{+/-}$ haploinsufficient and wild-type mice were obtained by breeding Pbx1$^{+/-}$ mice with wild-type animals (C57BL/6; Jackson Laboratory, Bar Harbor, ME). Generation of Sf-1$^{+/-}$ haploinsufficient animals has been described earlier (18).

For evaluation of adrenal morphology, expression studies and hormonal measurements, 10-wk-old female Pbx1$^{+/-}$ mice and wild-type controls were isolated and kept in a quiet environment overnight. Blood samples for hormonal measurements (n = 6 per genotype) were obtained by retroorbital bleeding after isoflurane anesthesia for restrained stress and ACTH-stimulated experiments and trunk blood collection for baseline measurements. In all instances, blood collection was done within 60 sec after initial mouse handling. Restrained stress was induced by placing the animals in a 50-ml Falcon tube for 30 min. ACTH stimulation was performed after injection of weight-adjusted doses of ACTH and blood collection after 30 min as described earlier (19). After microdissection, adrenals were measured and the tissues were snap frozen for protein/RNA extraction and *in situ* hybridization or immersed in paraformaldehyde for 3 h for histological analysis.

Downloaded from endo.endojournals.org by on February 21, 2008

For compensatory adrenal growth experiments, 9-wk-old male Pbx1$^{+/-}$ or wild-type mice were subjected to left-sided adrenalectomy (n = 6 per genotype) on d 0 following standard procedures as described earlier (20). Mice were euthanized on d 3, and the remaining adrenals were collected. All adrenal weights were measured after careful microdissection.

For real-time expression analysis of Pbx1, 8-wk-old female Sf-1$^{+/-}$ animals and age-matched wild-type controls (n = 3 each) were used with adrenals snap frozen after microdissection.

Adrenal morphology

For morphological evaluation, tissues were dehydrated, embedded in paraffin, sectioned, and stained with hematoxylin and eosin following standard procedures. Hematoxylin- and eosin-stained adrenal sections from wild-type and Pbx1$^{+/-}$ mice were examined with a standard light microscope using ×400 magnification. Cell nuclei within the zona fasciculata of three independent sections from three different animals per group were counted under standardized conditions. Cell counts were expressed as cell number per high-power field. Morphometric analysis for quantification of the x-zone was performed on at least three individual mice per genotype as described earlier (20).

Immunohistochemistry

For immunohistochemical analysis, paraffin-embedded sections were rehydrated, blocked with 0.3% H_2O_2 in methanol for 10 min, and incubated with blocking buffer for 15 min. Primary antibodies [proliferating cell nuclear antigen (PCNA), 1:500 (Santa Cruz Biotechnology, Santa Cruz, CA); SF-1, 1:500 (K. Morohashi); PBX1, 1:100 (Abcam, Cambridge, UK); and 20α-hydroxysteroid dehydrogenase (20αHSD), 1:5000 (Y. Weinstein)] were incubated overnight at 4 C after dilution in blocking buffer containing 3% BSA (Roche Diagnostics, Mannheim, Germany), 5% goat serum (Jackson ImmunoResearch Laboratories, West Grove, PA), and 0.5% Tween 20. After rinsing for 15 min in PBS, secondary antibody (goat antirabbit biotinylated IgG; Vector Laboratories, Burlingame, CA) was applied for 30 min at room temperature. Bound primary antibody was detected using the Immunocruz Kit (Santa Cruz Biotechnology) according to the manufacturer's protocol.

Western blot analysis

Adrenals were sonicated on ice until tissue was disrupted in RIPA buffer (50 mM Tris, 150 mM sodium chloride, 1.0 mM EDTA, 1% Nonidet P40, and 0.25% sodium deoxycolate, pH 7.0) that was supplemented with complete protease inhibitor cocktail (Roche, Mannheim, Germany) and phosphatase inhibitor cocktail 1 (Sigma Chemical Co., St. Louis, MO). After incubation by rotating at 4 C for 1 h, followed by a centrifugation step at 10,000 × *g* at 4 C for 5 min, protein concentration was assessed using a protein assay (Bio-Rad, Munich, Germany). Then, 10 μg of the protein preparation was run on a 10% acrylamide gel at 110 V for 1 h and transferred to nitrocellulose at 120 mA for 1 h. The nitrocellulose was then incubated with 5% nonfat dry milk overnight at 4 C with either rabbit anti-PCNA antibody (Santa Cruz Biotechnology) at a dilution of 1:1000, rabbit anti-SF-1 antibody at 1:1500 (K. Morohashi), or chicken anti-IGF-I receptor antibody at 2 μg/ml (Upstate, Charlottesville, VA), respectively. The washed blots were then incubated with suitable secondary antibodies conjugated to horseradish peroxidase (sheep antimouse, donkey antirabbit, or rabbit antichicken, all from Amersham Biosciences, Little Chalfont, UK) at a dilution of 1:10,000 for 1 h at room temperature. Antibody binding to the membrane was visualized using the KPL Western Luminescence ECL plus (Amersham) chemiluminescent detection system. All immunoblots were performed on at least six different animals per genotype. Bands were quantified using volume quantification (Quantity one, version 4.2.0; Bio-Rad, Hercules, CA), and resulting values were expressed as percent changes compared with wild-type controls.

In situ hybridization

PCR was used to amplify fragments of the appropriate Hox genes from mouse adrenal cDNA. All fragments were chosen within an untranslated sequence that showed no significant homology to other members of the Hox family. Corresponding sequences were as follows: for A9 (accession no. NM 010456), bases 627–999; for B8 (accession no. NM 010461), bases 252–612; and for C8 (accession no. NM 010466), bases 1001–1430. PCR fragments were cloned into pGEM-T Easy (Promega, Madison, WI) and subsequently sequenced to confirm integrity. The plasmids were linearized, and nonradioactive sense and antisense riboprobes labeled with digoxigenin were synthesized using *in vitro* transcription using either T7 or SP6 RNA polymerase as previously described (21).

Adrenals from wild-type controls were frozen in isopentane cooled in dry ice, and 25-μm sections were cut using a cryostat. *In situ* hybridization was carried out essentially as previously described (21). For the sense controls, tissue sections were probed with a cocktail of all three probes mixed together in equal quantities. Detection of the probes was via an antidigoxigenin antibody (Roche) coupled with the Renaissance Tyramide Signal Amplification System (NEN Life Science Products, Boston, MA). The cell nuclei were counterstained with TOTO-3 (Molecular Probes, Eugene, OR) and the sections analyzed using confocal microscopy.

Immunoprecipitation

HEK293T cells were transfected with pcDNASf-1 and/or pcDNAP-bxHA using the calcium phosphate-mediated transfection method. After 24 h, cells were harvested by scraping them in a buffer containing 50 mM Tris-HCl, pH 8.0; 150 mM NaCl; 5 mM EDTA; 0.5% Nonidet P-40; 0.1 mM phenylmethylsulfonyl fluoride (22), and 100 mg protein was incubated at 4 C with 5 μl anti-Sf-1 (rabbit polyclonal; Upstate) or anti-HA (mouse monoclonal, 6E2; Cell Signaling, Danvers, MA). After 12 h, 25 μl packed protein A (Invitrogen, Carlsbad, CA) or protein G agarose beads (Sigma) were added and incubated at 4 C for another hour. After three consecutive washes with 1 ml IPH buffer, agarose beads were heated to 95 C in loading buffer containing SDS and mercaptoethanol for 5 min. Samples were subjected to 10% SDS-PAGE, transferred to nylon membrane (Bio-Rad) by semidry technique. Protein detection was conducted using anti-SF-1 (rabbit polyclonal) and anti-HA (rabbit polyclonal, Y11; Santa Cruz Biotechnology) and the West Dura extended duration kit (Pierce, Rockford, IL). Alternatively, instead of IPH buffer, experiments with immunoprecipitation were carried out in modified RIPA buffer and 1:1 PBS:modified RIPA buffer obtaining the same results.

RT-PCR

Individual adrenals from each group were used for RNA extraction using the QIAGEN (Valencia, CA) RNA mini kit following the instructions of the manufacturer. cDNA was created using a RT kit (Promega) and 1.0 μg total RNA. Aliquots of the cDNA samples were subjected to the subsequent PCR, which were performed with primer pairs and annealing temperatures as given in supplemental Table 1. For detection of Hox gene products, identical primers as for the generation of the *in situ* probes were used. Amplification products were separated on 1% agarose gel and stained with ethidium bromide.

Real-time PCR

IGF system, Pcna, and Sf-1 in vivo. Quantification of mRNA abundance was performed by real-time PCR detection using an ABI PRISM 7700 Sequence Detector (PE Biosystems, Weiterstadt, Germany) and Sybr Green as a double-stranded DNA-specific fluorescent dye. Amplification mixes (25 μl) contained 2.5 μl cDNA solution, 2× Sybr Green PCR Master Mix, 12.5 pM of each primer, and 0.25 IU AmpErase uracil *N*-glycosylase (PE Biosystems). Amplification primers (Table 1) were designed using the Primer Express software (PE Biosystems). PCR was started with 2 min at 50 C for AmpErase activation and 10 min at 95 C for denaturation. The program continued with 40 cycles of 15 sec at 95 C and 60 sec at 60 C. The amplicons were verified by sequence determination. Each assay included triplicates of cDNA for the gene of interest, no-template control and four dilutions of cDNA pooled from all genetic groups for the gene of interest and for the reference gene β-actin to calculate the corresponding amplification efficiency ($E = 10^{-(1/b)} - 1$; b is the regression coefficient). The parameter CT

Downloaded from endo.endojournals.org by on February 21, 2008

TABLE 1. Primer sequences and annealing temperatures used for real-time PCR

Amplification product	Sequence	Nucleotides	Annealing temperature (C)
20-αHSD (fwd)	GTACAAGCCTGTGTGCAACCA	582–686	60
20-αHSD (rev)	TCTTCTGGTTGCCTATGGTGC		
β-actin (fwd)	ACCCCAGCCATGTACGTAGC	465–565	60
β-actin (rev)	CTCTGCCCCAGTGGGTGTG		
FGF-15 (fwd)	CAGAACTGAGAGCCAGGAGC	1095–1545	62
FGF-15 (rev)	CAAAGCCAAAAGGCTGAAAG		
IGF-I (fwd)	ATGAGTGTTGCTTCCGGAGCT	272–352	60
IGF-I (rev)	GGATGTTTTCGTCGGGCGA		
IGF-II (fwd)	GCATGCTTGCCAAAGAGCTC	450–550	60
IGF-II (rev)	TGCCCCCTCGGAGAAGC		
IGF-I-R (fwd)	CCGCGCCAGTTTTGATG	4026–4098	60
IGF-I-R (rev)	TTGCTCTCCCGGAACGGA		
IGFBP-2 (fwd)	GCGCGGGTACCTGTGAAA	403–482	60
IGFBP-2 (rev)	CTACTGCTGGTGAGACTCCCT		
IGFBP-3 (fwd)	CCTCCGAGTCTAAGCGGGAG	686–786	60
IGFBP-3 (rev)	TACACGACTCAGGGTCTCCG		
IGFBP-5 (fwd)	CTGCCCACCCCAGAGTCAT	575–675	60
IGFBP-5 (rev)	GGGAGGTCCTCAAGTTTCGG		
MC2-R (fwd)	CTGCCACGAGGCTTAAGATAAC	663–1150	58
MC2-R (rev)	GCCTGTCAAGCATTAGTGACAA		
Pbx1 (fwd)	GGGTGCAGGTTCAGACAACT	302–711	58
Pbx1 (rev)	CGCACTTCTTGGCTAACTCC		
PCNA (fwd)	ATCAATGAGGCCTGCTGGG	196–296	60
PCNA (rev)	CTTACTCTGCGCTCCGAAGG		
SF-1 (fwd)	TGCACTGCAGCTGGACCGCCAGGAGTT	1248–1638	58
SF-1 (rev)	AGGGCTCCTGGATCCCTAATGCAAGGA		
StAR (fwd)	GACCTTGAAAGGCTCAGGAAGAAC	7–938	58
StAR (rev)	TAGCTGAAGATGGACAGACTTGC		

Nucleotide positions are given relative to the start codon of the respective open reading frame. fwd, Forward, 5′–3′; rev, reverse, 3′–5′. For further details, see text.

(threshold cycle) is defined as the cycle number at which fluorescence intensity exceeds a fixed threshold. Relative mRNA expression for each gene of interest (I) was calculated using the formula: $(1 + E_{[I]})^{-CT[I]}/(1 + E_{[\beta\text{-actin}]})^{-CT[\beta\text{-actin}]}$. Data were analyzed using the Student's *t* test and correlation analysis (Pearson).

In vitro Sf-1-Pbx1 interaction, Pbx1, and Mc2-r in vivo. For these sets of experiments, real-time PCR was performed using the FastStart DNA MasterPlus SYBR Green I reaction mix in the LightCycler 1.5 (Roche). Real-time PCR conditions were preincubation at 95 C for 10 min followed by amplification of 40–45 cycles at 95 C for 10 sec, the annealing temperature (primer dependent as given in Table 1) for 6 sec, and extension at 72 C, at which the time is calculated by the product length in base pairs divided by 25 (Roche, Indianapolis, IN). The melting curve analysis was performed between 65 and 95 C (0.1 C/sec) to determine the melting temperature of the amplified product and to exclude undesired primer dimers. Furthermore, the products were run on a 1% agarose gel to verify the amplified product. Quantification was adjusted using the housekeeping gene β_2-microglobulin. To facilitate overall comparison of individual real-time experiments, expression levels of the particular genes were set as 100% for wild-type animals.

For evaluation of endogenous gene expression after forced overexpression of Sf-1 and Pbx1, cells were harvested 48 h after transfection, and real-time analysis was performed as described.

Reporter gene assays

A 2.7-kb fragment of the murine 5′ untranslated region of the Pbx1 gene was PCR cloned using primers 5′-PBX1prom-3, TTC CCA CTT GGC GAA AAG AAA TCA GAG CC, and 3′-PBX1prom-3, CCA GAA CCA ATC TGT CCT TCA AAC TGC CTC, from mouse genomic DNA using the Expand Long Template PCR System (Roche, Indianapolis, IN). Cycling conditions and procedure were performed according to the manufacturer's protocol. The PCR product was first cloned into pCR2.1 vector using TA cloning kit (Invitrogen, Karlsruhe, Germany) and subsequently subcloned into the pGL2 basic vector (Promega).

In addition, a full-length promoter construct of the ACTH receptor (Mc2-r) and a construct with three mutated Sf-1-binding sites that have been described previously (23) as well as an artificial Sf-1-responsive element consisting of multiple core Sf-1-binding sites from the 21-OH genes fused to −36 PRL-LUC (kindly provided by Dr. K. Parker) were used. For stimulation, expression vectors for the full-length murine Pbx1a and Sf-1 were used, respectively.

Mouse adrenocortical Y1 cells were grown to a density of 100,000 per 24-well plate in Ham's F-10 medium with 7.5% horse serum and 2.5% fetal bovine serum and transiently transfected using ExGen 500 (MBI Fermentas, St. Leon-Rot, Germany) for 5 h according to the manufacturer's instructions with 250-ng expression vectors (if not stated otherwise) and 500-ng promoter constructs, respectively. Total amount of transfected DNA was kept constant to 1 μg by adding empty pcDNA expression vector. At 48 h after transfection, cells were harvested and luciferase activity was measured (Luciferase Reporter Gene Assay; Roche, Mannheim, Germany). Luciferase values were normalized for total protein content. Each data point represents at least four independent measurements.

Plasma hormone measurements

Plasma corticosterone was measured using a commercially available RIA (MP Biomedicals, Eschwege, Germany). Plasma ACTH was determined with an immunoradiometric assay (Immuno Biological Laboratories, Hamburg, Germany). All assays were performed according to the manufacturers' protocols. The intra- and interassay coefficients of variation were less than 10% and less than 7%, respectively, for all assays. All hormone measurements were performed on six animals per genotype on single aliquots due to the small amount of plasma available.

Statistical analysis

All results are expressed as mean ± SEM. If not stated otherwise, all statistical comparisons were analyzed by ANOVA and Fisher's protective least significant difference test. Statistical significance is defined as $P < 0.05$ and is indicated by *asterisks* in the figures.

Downloaded from endo.endojournals.org by on February 21, 2008

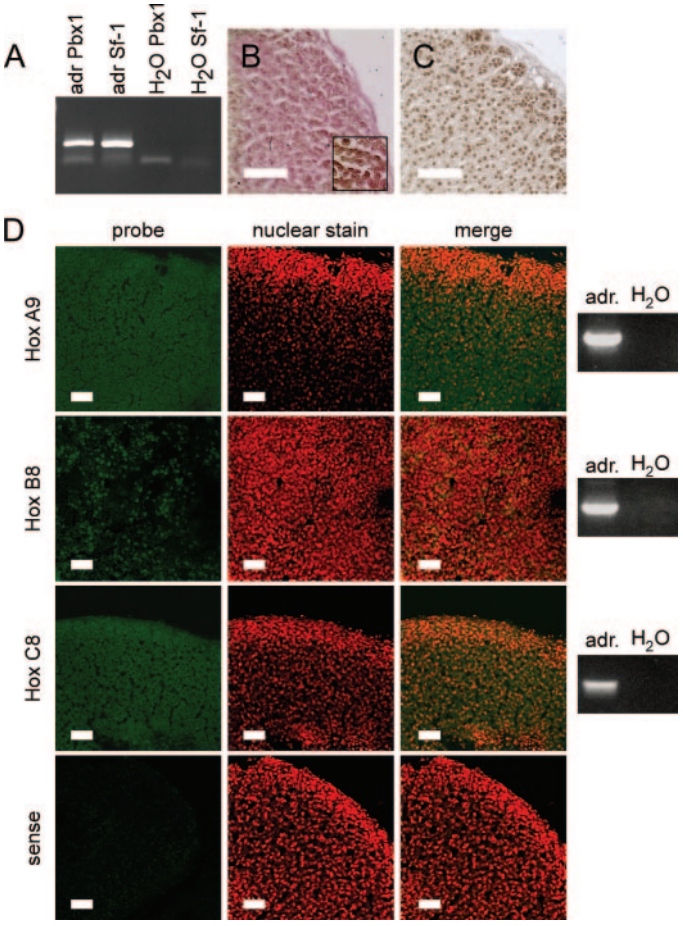

FIG. 2. Adrenal expression pattern of Pbx1, Sf-1, and Hox genes. Expression of Pbx1 (A and B) and Sf-1 (A and C) in the adult adrenal cortex was detected by RT-PCR and immunohistochemistry. Moreover, expression pattern of HoxA9, HoxB8, and HoxC8 was investigated by *in situ* hybridization and RT-PCR, indicating expression of the Hox genes in all zones of the murine adrenal cortex (D). In contrast, no specific staining was evident using a mixture of sense probes of each individual Hox gene (D, sense).

Results

Pbx1, Hox genes, and Sf-1 are constitutively expressed in the adrenal cortex of the adult mouse

Expression of the transcription factors Pbx1 and Sf-1 was detectable in the adrenal cortex on the mRNA level (Fig. 2A) as well as by immunohistochemistry (Pbx1, Fig. 2B; Sf-1, Fig. 2C). Moreover, major Pbx1 binding partners such as Hox A9, B8, and C8, which are essential mediators of Pbx1 action (2, 24–26), were also present in the adrenal cortex by means of *in situ* hybridization and RT-PCR analysis (Fig. 2D). These results provided the rationale for investigating the effects of Pbx1 haploinsufficiency on the adrenal cortex.

Pbx1 haploinsufficient mice are characterized by lower adrenal weights with smaller x-zone but adrenocortical hypertrophy

$Pbx1^{+/-}$ animals displayed smaller adrenals (Fig. 3B) resulting in a significantly lower adrenal weight (4.4 ± 0.4 mg) in comparison with wild-type controls (7.5 ± 0.3 mg, $P <$ 0.0001; Fig. 3, A and C). Despite the lower adrenal weight, morphometric analyses demonstrated hypertrophy of the zona fasciculata as indicated by a lower cell number per high-power field in $Pbx1^{+/-}$ mice (63.0 ± 3.3%; Fig. 3, E and F) than in wild-type animals (89.3 ± 8.3%, $P = 0.014$; Fig. 3, D and F).

In contrast, morphological studies based on the x-zone-specific expression pattern of 20αHSD (Fig. 3, G and H) suggested a decrease in the size of the x-zone in nulliparous female mice in the context of Pbx1 haploinsufficiency (Fig. 3H) in comparison with wild-type controls (Fig. 3G). These observational findings could be verified by morphometric analysis (ratio x-zone area/whole adrenal cortex area, 100.0 ± 6.3 *vs.* 57.3 ± 13.9%, $P < 0.05$; Fig. 3I).

Pbx1 haploinsufficiency is associated with lower adrenal cellular proliferation, decreased compensatory adrenal growth, and changes of expression in the IGF system

Because the observed lower adrenal weight in $Pbx1^{+/-}$ animals could have been explained by a proliferation defect, detailed expression analysis of the proliferation marker Pcna was performed. Indeed, Pbx1 haploinsufficient mice displayed a marked reduction in adrenal expression levels of Pcna, which was observed in real-time PCR (52.3 ± 12.5 *vs.* 100 ± 7.6%, $P = 0.01$; Fig. 4A), Western blot analysis (Fig. 4B), and immunohistochemistry (Fig. 4C).

To further substantiate these findings on adrenocortical proliferation under baseline conditions, we used the well-defined growth paradigm of compensatory adrenal growth after unilateral adrenalectomy (27). In accordance with the results from female animals, adrenal weights in male mice at baseline were significantly lower in $Pbx1^{+/-}$ mice in comparison with wild-type controls (1.6 ± 0.1 *vs.* 2.1 ± 0.1 mg, $P < 0.002$). Moreover, unilateral adrenalectomy resulted in a blunted compensatory growth of the contralateral adrenal in $Pbx1^{+/-}$ animals (1.7 ± 0.1 mg, $P = 0.65$ *vs.* baseline) in contrast to wild-type mice that showed the expected increase in adrenal weight (2.7 ± 0.1 mg, $P < 0.001$ *vs.* baseline; Fig. 4D).

Because the IGF system is a major determinant of adrenocortical growth in adrenal physiology and tumorigenesis, this system was investigated thoroughly by real-time analysis. Although IGF-I and IGF-II expression levels were not different between the two genotypes, IGF-I receptor was significantly down-regulated (46 ± 6 *vs.* 100 ± 10%, $P =$ 0.007). Furthermore, IGF-binding protein 2 (IGFBP-2) was up-regulated about 10-fold (1033.0 ± 408.5 *vs.* 100 ± 8.3%, $P = 0.04$), whereas IGFBP-3 and IGFBP-5 expression levels remained unaltered by Pbx1 haploinsufficiency (Fig. 4E). In accordance with the lower IGF-I receptor mRNA expression levels, adrenals from $Pbx1^{+/-}$ also displayed lower IGF-I receptor protein levels by means of Western blot analysis (67.3 ± 4.1 *vs.* 100.0 ± 7.8%; $P = 0.03$; Fig. 4E, *inset*).

Taken together, these findings indicate that a full complement of Pbx1 is indispensable for proper growth and proliferation of the adrenal cortex. In addition, the transcriptional modulation of the intraadrenal IGF system associated with Pbx1 haploinsufficiency might contribute to the observed adrenal growth defect.

Downloaded from endo.endojournals.org by on February 21, 2008

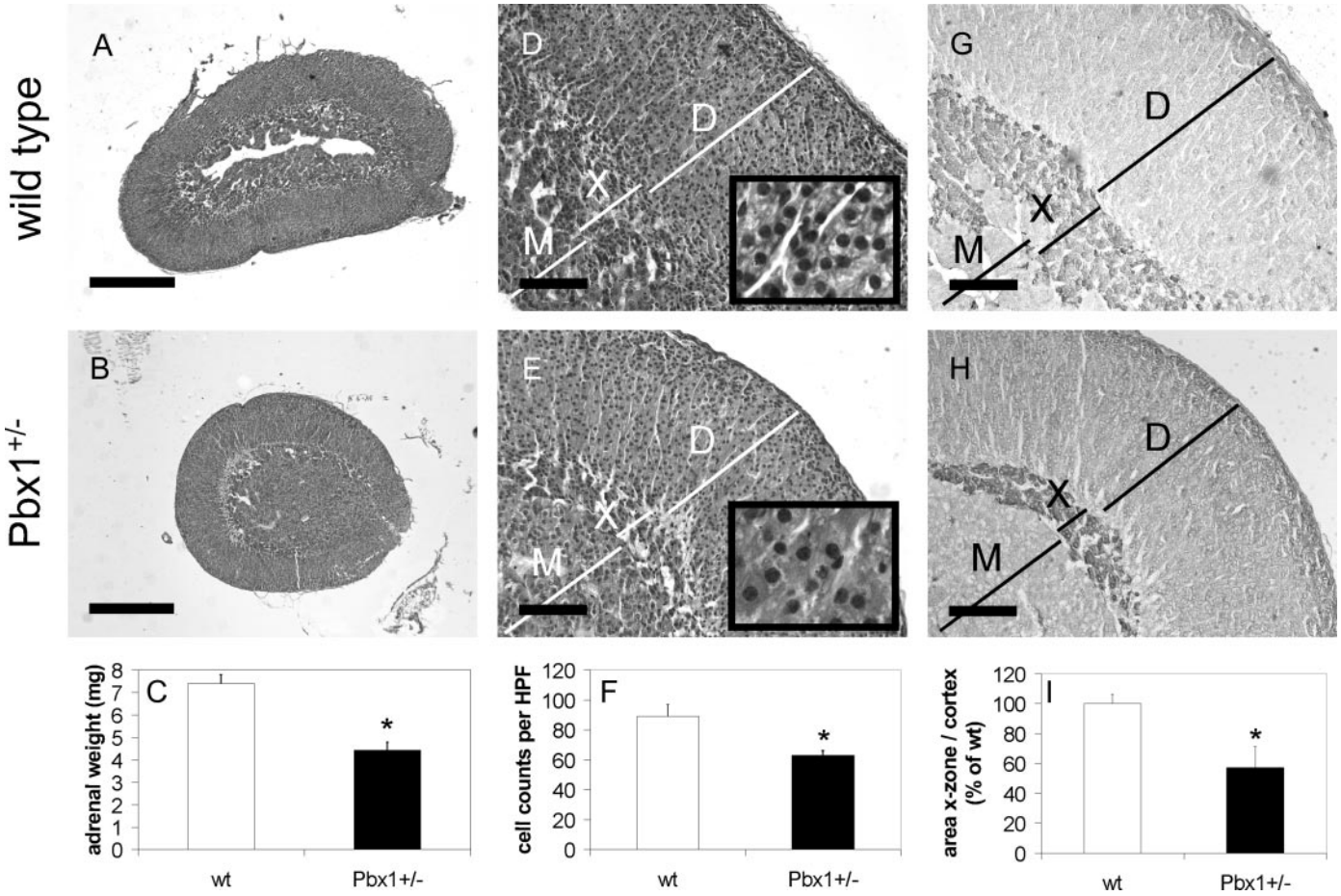

FIG. 3. Adrenal phenotype of female Pbx1 heterozygous animals. Female Pbx1$^{+/-}$ mice were characterized by smaller adrenals (B) with significant lower adrenal weights (C) in comparison with wild-type controls (A), whereas lower cell number per high-power field within the zona fasciculata (F) indicated cellular hypertrophy in Pbx1$^{+/-}$ mice (E) compared with wild-type animals (D). Expression pattern of the x-zone-specific marker 20αhsd (G and H) gave evidence for a smaller x-zone in Pbx1$^{+/-}$ mice (H) in comparison with wild-type controls (H) that was quantified by x-zone morphometry verifying smaller x-zone area in Pbx1 heterozygous animals (I). *Bars* for low- and high-power magnification represent 500 and 100 μm, respectively. D, Definitive zone; M, medulla; X, x-zone.

Pbx1 haploinsufficient mice have a blunted steroid response after stimulation

On a functional level, baseline corticosterone levels were similar in Pbx1$^{+/-}$ (18.8 ± 6.2 ng/ml) and wild-type (16.7 ± 4.7 ng/ml, $P = 0.8$) animals. In contrast, corticosterone stimulation was significantly blunted in Pbx1$^{+/-}$ mice after ACTH administration (184.4 ± 57.6 ng/ml *vs.* wild-type 358.8 ± 28.3 ng/ml, $P = 0.03$), whereas no statistical difference could be observed after restrained stress experiments (375.0 ± 36.3 ng/ml *vs.* wild-type 495.9 ± 51.2 ng/ml, $P = 0.14$; Fig. 5). Accordingly, basal ACTH levels were similar between the two groups (259.0 ± 25.2 pg/ml *vs.* wild-type 296.0 ± 37.0 pg/ml, $P = 0.60$) but significantly higher in Pbx1$^{+/-}$ mice after restrained stress (1177.5 ± 57.8 pg/ml *vs.* wild-type 797.3 ± 112.8 pg/ml, $P = 0.02$; Fig. 5). Collectively, these data correspond with a compensated primary adrenal insufficiency in Pbx1 haploinsufficient mice.

Pbx1 and Sf-1 induce promoter activation of the ACTH receptor without evidence for direct physical interaction

Consistent with the hormonal data suggesting a decreased responsiveness of the adrenal cortex to ACTH expression levels of the ACTH receptor [melanocortin receptor (Mc2-r)] were significantly lower in Pbx1$^{+/-}$ animals (77.7 ± 7.9%) in comparison with wild-type controls (100 ± 2.8%, $P = 0.02$; Fig. 6A). Therefore, we further evaluated possible direct interaction of Pbx1 on the transcriptional regulation of the Mc2-r. In addition to the three well-characterized Sf-1-binding sites within the Mc2-r promoter (28), sequence analysis predicted two potential Pbx1/Hox and two potential Pbx1/Meis binding sites, displaying the consensus TGATNNAT (29) and TGACAG (30) at positions −63 to −56, −326 to −319, −686 to −681, and −915 to −910 bp, respectively. Accordingly, promoter studies using a full-length Mc2-r promoter construct revealed a significant increase in promoter activation by Pbx1 (342.0 ± 81.2% *vs.* pcDNA 100 ± 4.7%, $P = 0.007$) which was of similar magnitude as that induced by Sf-1 (520.8 ± 121.3 *vs.* 100 ± 4.7%, $P = 0.002$). In addition, overexpression of Pbx1 together with Sf-1 resulted in an additional significant increase in Mc2-r promoter activity over Sf-1 alone (1627.4 ± 408.2 *vs.* 520.8 ± 121.3%, $P < 0.001$; Fig. 6B).

Using the full-length Mc2-r promoter with mutated SF-1-binding sites at positions −35, −98, and −209, no significant

Downloaded from endo.endojournals.org by on February 21, 2008

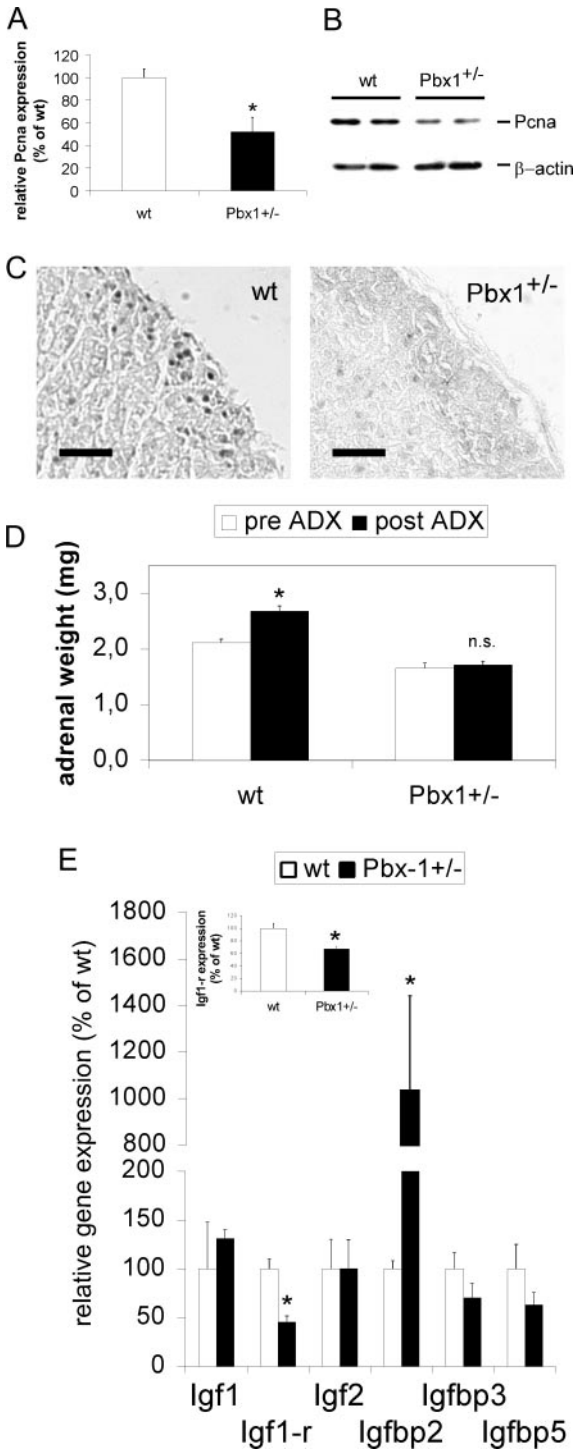

FIG. 4. Pbx1 haploinsufficiency results in an adrenal proliferation defect. Adrenal expression of the proliferation marker Pcna was reduced by means of RT-PCR analysis (A), immunoblotting (B), and immunohistochemistry (C) in the context of Pbx1 haploinsufficiency. In addition, compensatory adrenal growth after unilateral adrenalectomy was blunted in male Pbx1$^{+/-}$ mice in comparison with wild-type controls (D). Expression analysis of members of the IGF system by real-time PCR (E) revealed significantly decreased adrenal expression of IGF-I receptor (Igf1-r) and marked up-regulation of IGFBP-2 mRNA levels in Pbx1$^{+/-}$ animals. Accordingly, IGF-I receptor protein levels were significantly diminished in adrenals from in Pbx1$^{+/-}$ mice (E, *inset*). *Bars* for immunohistochemistry represent 50 μm. ADX, Unilateral adrenalectomy.

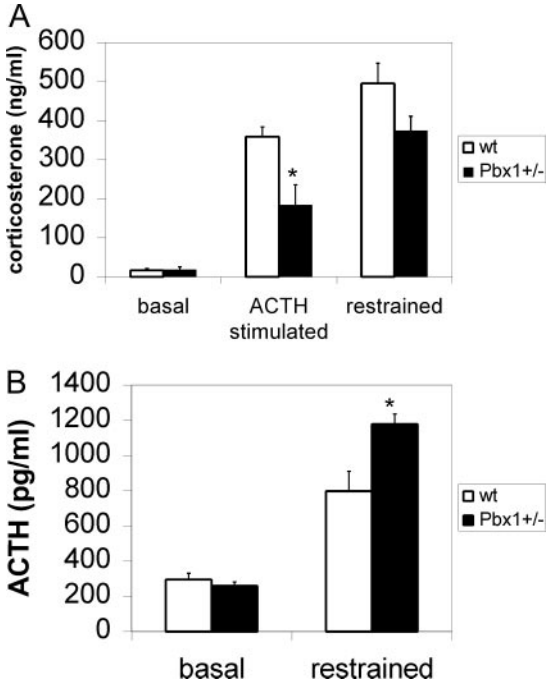

FIG. 5. Pbx1 haploinsufficiency is accompanied by compensated primary adrenal insufficiency. Although baseline ACTH and corticosterone levels were not different between wild-type animals and Pbx1$^{+/-}$ mice (A and B), ACTH stimulation resulted in a blunted adrenal corticosterone response in Pbx1$^{+/-}$ mice in comparison with wild-type controls (A). In contrast, stress-induced ACTH levels were significantly elevated in Pbx1$^{+/-}$ mice indicating compensatory increase in ACTH secretion (B).

Sf-1 response was detectable (133.4 ± 3.7 *vs.* 100 ± 11.0%, $P = 0.14$), whereas Pbx1-dependent effects on the promoter activity remained intact either alone (169.1 ± 17.2 *vs.* 100 ± 11.0%, $P = 0.01$) or in combination with SF-1 (232.9 ± 20.6 *vs.* 100 ± 11.0%, $P < 0.001$; Fig. 6C).

Using an artificial Sf-1 promoter construct, which consisted of multiple isolated Sf-1-binding sites, only Sf-1-dependent effects on promoter activation were evident (Sf-1 alone, 433.9 ± 13.8 *vs.* 100 ± 8.2%, $P < 0.001$; Pbx1 plus Sf-1, 370.4 ± 16.5 *vs.* 100 ± 8.2%, $P < 0.001$), whereas Pbx1 was not able to significantly increase promoter activity over baseline (94.6 ± 8.8 *vs.* 100 ± 8.2%, $P = 0.76$) or over Sf-1-dependent activation alone (370.4 ± 16.5 *vs.* 433.9 ± 13.8%, $P = 0.07$), respectively (Fig. 6D).

Collectively, these data demonstrate that Pbx1 and Sf-1 have additive effects on Mc2-r promoter activity. Moreover, Sf-1 seems not to be required for Pbx1 to evoke its activating effects on the Mc2-r promoter. Conversely, Pbx1 fails to increase Sf-1-dependent effects on promoter activation in the absence of Pbx1-binding sites.

Because a functional interaction between Pbx1 and Sf-1 could require direct protein-protein binding, we performed immunoprecipitation experiments under various conditions (Fig. 6E and data not shown). However, overexpression of Sf-1 was not able to coprecipitate Pbx1, suggesting that direct interaction between the two transcription factors seems not to play a major role for the observed functional effects on promoter activation.

Downloaded from endo.endojournals.org by on February 21, 2008

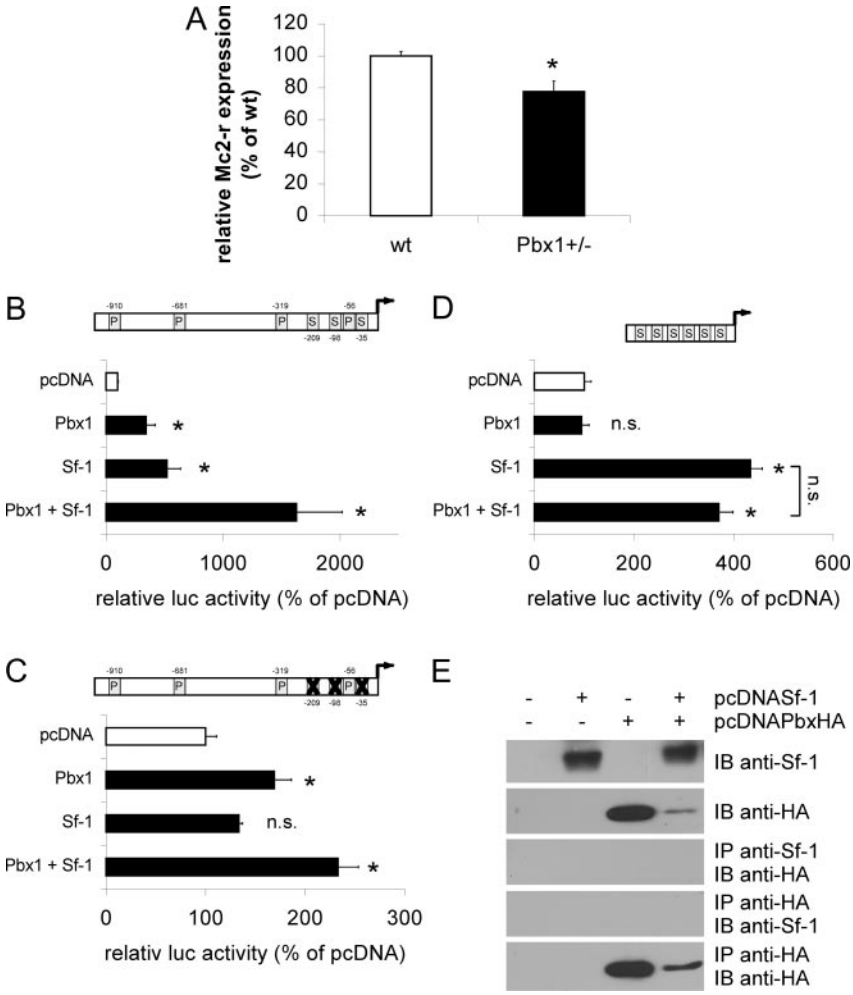

FIG. 6. Pbx1 and Sf-1 independently up-regulate expression of the ACTH receptor (Mc2-r). *In vivo*, adrenal Mc2-r expression was significantly lower in Pbx1$^{+/-}$ mice in comparison with wild-type controls (A). Using a full-length Mc2-r promoter construct, both Pbx1 and Sf-1 led to a significant increase in promoter activity (B). Moreover, Pbx1 and Sf-1 in combination resulted in an additional significant increase over promoter activity induced by Sf-1 alone (B). In contrast, a Mc2-r promoter construct with mutated Sf-1-binding sites could only be stimulated by Pbx1, whereas no further activation was evident by Sf-1 (C). Conversely, using an artificial Sf-1-responsive promoter construct, Pbx1 did not increase promoter activity (D). However, no direct protein-protein interaction between Pbx1 and Sf-1 could be established by immunoprecipitation experiments (E). S and P in schematic promoter constructs denote Sf-1-binding sites and consensus Pbx1-binding sites, respectively.

Pbx1 does not affect Sf-1 expression levels in adrenocortical tumor cell lines in vitro and in adult adrenal glands in vivo

Expression of Fgf15, which represents a direct downstream target of Pbx1 action (31), was up-regulated by overexpression of Pbx1 in Y1 cells in a dose-dependent manner (247.4 ± 29.8% for 1000 ng Pbx1 *vs.* 100 ± 1.7% for pcDNA, $P = 0.03$; Fig. 7A). In contrast, endogenous Sf-1 expression levels remained unchanged (119.4 ± 2.4% for 1000 ng Pbx1 *vs.* 100 ± 6.6%, $P = 0.12$; Fig. 7C) under the same experimental conditions. Concomitantly, Sf-1 expression levels in adrenal glands of wild-type and heterozygous Pbx1 mice were assessed by real-time PCR and Western blot analysis. In accordance with the *in vitro* data, Sf-1 expression in adult adrenals on mRNA (115.3 ± 17.0 *vs.* 100 ± 6.6%, $P = 0.39$; Fig. 7D) or protein level (102.5 ± 7.3 *vs.* 100 ± 14.5%, $P = 0.90$; Fig. 7E) was not significantly different in Pbx1$^{+/-}$ mice in comparison with wild-type controls.

Sf-1 induces Pbx1 promoter activation in vitro and in vivo

Upon overexpression of Sf-1 in Y1 cells, the direct Sf-1 target gene mStAR (170.5 ± 18.6 *vs.* 100 ± 9.4%, $P < 0.001$; Fig. 7E) as well as endogenous Pbx1 (165.65 ± 19.4% *vs.* 100 ± 11.6%, $P = 0.01$; Fig. 7F) were significantly up-regulated in the Sf-1-transfected cells, indicating Sf-1-dependent activation of endogenous Pbx1 transcription.

In accordance with these *in vitro* findings in Y1 cells, sequence analysis of the Pbx1 promoter predicted four potential Sf-1-binding sites represented by a CAAGG consensus sequence (positions −11 to −15 and −2465 to −2454) and AGGTCA consensus sequence (32) (positions −2465 to −2460 and −2312 to −2307). Notably, four consensus binding sites for Pbx1 were also evident within the Pbx1 promoter region (−1942 to −1933, −982 to −975, −639 to −632, and −535 to −542) by sequence analysis. Functional significance of these findings was verified by Pbx1 promoter stimulation studies. In accordance with the sequence analysis, overexpression of Sf-1 resulted in a dose-dependent increase in Pbx1 promoter activation (125 ng Sf-1, 157.7 ± 6.9%, $P = 0.017$; 250 ng Sf-1, 188.4 ± 8.9%, $P = 0.014$; 500 ng Sf-1, 272.2 ± 17.0%, $P < 0.001$ *vs.* pcDNA, 100 ± 4.7%; Fig. 7G). Furthermore, Pbx1 promoter activity was also significantly induced by Pbx1 overexpression (331.1 ± 24.0 *vs.* 100 ± 4.7%, $P < 0.001$; Fig. 7G). *In vivo*, adrenal glands of Sf-1 heterozygous animals showed significantly lower Pbx1 levels on the mRNA level (43.3 ± 15.3 *vs.* 100 ± 12.7%, $P = 0.047$; Fig. 7H). Taken together, these data are in agreement with the concept of an Sf-1-dependent promoter activation of Pbx1.

Downloaded from endo.endojournals.org by on February 21, 2008

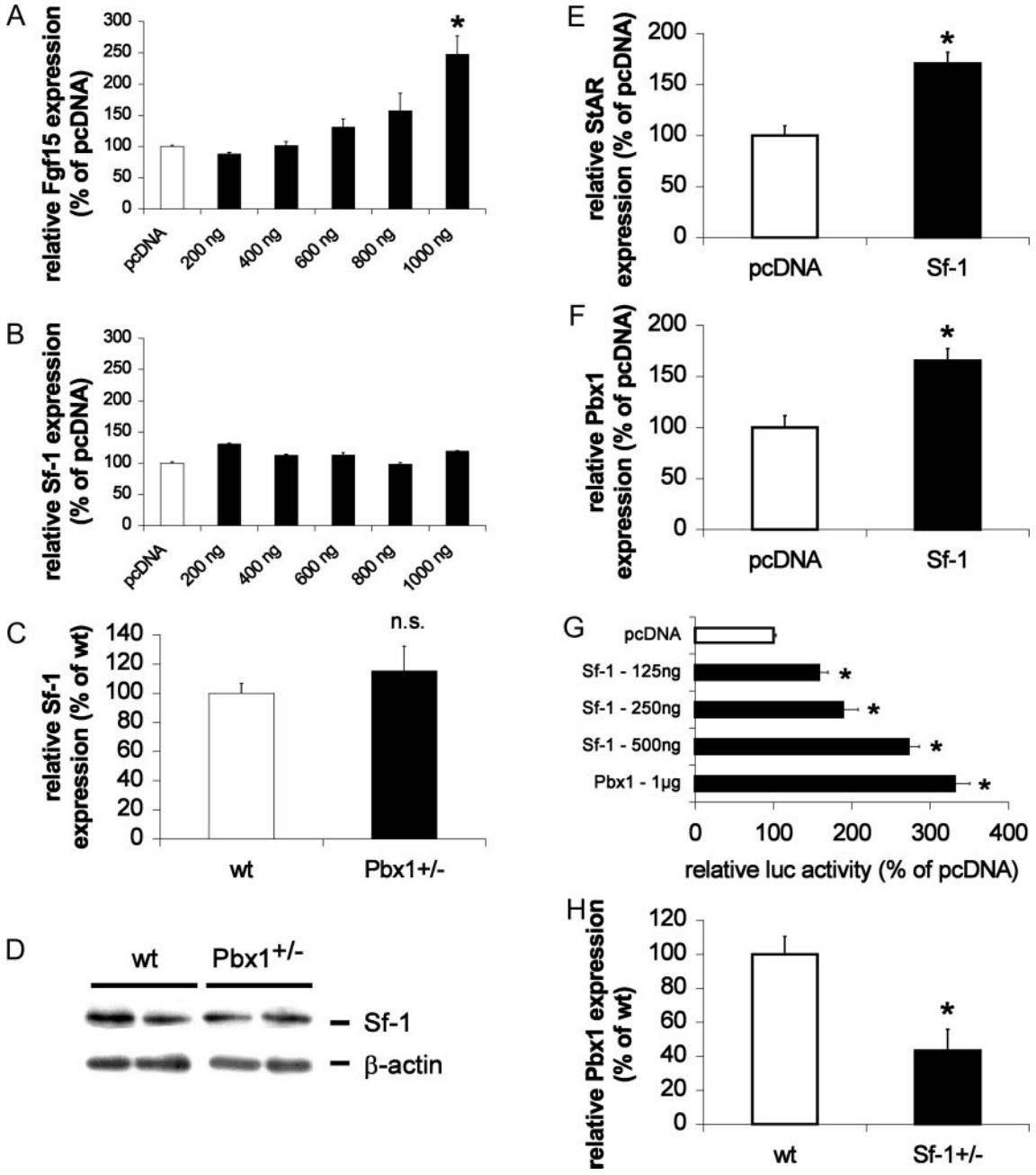

FIG. 7. Transcriptional interdependence between Pbx1 and Sf-1. Although overexpression of Pbx1 in Y1 cells resulted in a significant upregulation of the Pbx1 downstream target Fgf15 in a dose-dependent manner (A), endogenous Sf-1 levels were not affected by Pbx1 overexpression (B). Accordingly, Pbx1 haploinsufficiency did not significantly alter adrenal Sf-1 mRNA levels (C) or protein expression (D) *in vivo*. In contrast, overexpression of Sf-1 in Y1 cells led to increased mRNA levels of the Sf-1-dependent downstream target StAR (E) as well as endogenous Pbx1 (F). Moreover, Pbx1 promoter activity was significantly increased by Sf-1 in a dose-dependent manner as well as by Pbx1 itself (G). Likewise, *in vivo* adrenal expression levels of Pbx1 were significantly decreased in Sf-1 haploinsufficient animals (Sf-$1^{+/-}$) compared with wild-type controls (H).

Discussion

Regulation and maintenance of adrenocortical growth and steroidogenesis is dependent upon extraadrenal peptide hormones as well as the presence of intraadrenal transcription factors. The adrenal phenotype in Pbx1 haploinsufficient animals with lower adrenal weight, lower basal proliferation, and lack of compensatory adrenal growth as well as blunted steroid output upon stimulation demonstrates the requirement of a full complement of Pbx1 for proper adrenocortical growth and function. Notably, these defects in adrenocortical cellular proliferation and steroidogenesis recapitulate the phenotype as observed in Sf-1 heterozygous knockout mice (20, 33).

The observed decrease in the cell number per high-power field in $Pbx1^{+/-}$ mice indicating cellular hypertrophy of the zona fasciculata clearly does not explain the concomitant re-

Downloaded from endo.endojournals.org by on February 21, 2008

duction in adrenal weight. However, similar phenotypic changes have been demonstrated in Sf-1 haploinsufficient mice (19, 20, 33) and have been interpreted as the consequence of latent primary adrenal insufficiency with consecutively elevated levels of ACTH and other proopiomelanocortin-derived peptides together with intracellular compensatory mechanisms including up-regulation of the orphan nuclear receptor nerve growth factor-induced B (NGFI-B) (34). Likewise, although a smaller x-zone might contribute to the observed decrease in adrenal weight in virgin female animals, it does not explain the lower adrenal weight in postpubertal male mice with already regressed x-zone. As such, cellular hyperplasia of the zona fasciculata or differences in zonation seem not to be major determinants of the observed adrenal growth defect.

The adrenal cortex is a dynamic organ with constant cellular replacement from the proposed subcapsular stem cell zone and inward migration of newly differentiated daughter cells (35, 36). As such, growth and adaptation of the adult adrenal cortex is dependent upon the proliferative potential of this stem cell population. Thus, the observed lower levels of the proliferation marker PCNA as detected by RT-PCR, Western blot analysis, and immunohistochemistry suggest a crucial role of Pbx1 for the regulation of adrenocortical stem cell proliferation. In keeping with these findings, severe adrenal hypoplasia has been described in $Pbx1^{-/-}$ embryos (15), which parallels the defects in proliferation of progenitor cells previously reported in other organ systems (7, 10). The lack of compensatory growth in $Pbx1^{+/-}$ animals resembles that of Sf-1 heterozygous mice (20) and provides additional evidence that Pbx1 is indispensable for the maintenance of the adrenal cortex in the adult animal.

IGF-II is considered one of the most potent growth factors for the adrenal cortex in the context of both adrenal development (37) and adrenal tumorigenesis (38). Genetic studies on adrenocortical carcinomas have demonstrated a variety of genetic changes resulting in IGF-II overexpression. Therefore, we hypothesized that alteration in the local IGF system might play a role in the observed lower proliferation at baseline and upon stimulation. Indeed, although no changes in expression levels of IGF-I or IGF-II are evident in adrenals from $Pbx1^{+/-}$ animals, adrenal IGF-I receptor expression is significantly down-regulated, whereas IGFBP-2 expression levels are considerably higher in $Pbx1^{+/-}$ mice. These descriptive data on expression levels in a complex and dynamic *in vivo* system have to be interpreted with caution. However, because the main effects of IGF-I in the adrenal cortex are mediated by the IGF-I receptor and IGFBP-2 has been demonstrated to modulate IGF-I-dependent action on the adrenal cortex (39), both changes in expression levels could contribute to the evident proliferation defect.

Development of the adrenal cortex and functional maintenance in the adult organism is dependent upon an intact hypothalamus-pituitary-adrenal axis, in that a lack of pituitary proopiomelanocortin causes severe adrenal hypoplasia (40). The Mc2-r is a central part of the hypothalamus-pituitary-adrenal axis by mediating the adrenal steroid output in response to pituitary ACTH (41). As such, the observed lower adrenal expression levels of the Mc2-r are in line with the blunted adrenal responsiveness to ACTH *in vivo* in Pbx1 haploinsufficient animals.

In addition to its well described binding sites for Sf-1 (23, 28), the Mc2-r promoter contains four binding sites for Pbx1/Hox and Pbx1/Meis heterodimers, respectively. Interestingly, the proximal promoter fragment from position −12 to −109 contains one Pbx1/Hox-binding site that is flanked by two Sf-1-binding sites in close proximity. This promoter sequence is highly conserved between *Homo sapiens* and *Mus musculus*, displaying about 80% sequence similarity. Because these findings gave indirect evidence for the functional relevance of these transcription factors for Mc2-r regulation, we used the Mc2-r promoter as a model for Pbx1- and Sf-1-dependent promoter activation. In fact, Pbx1 results in an increase in baseline as well as Sf-1-stimulated promoter activity of the Mc2-r promoter, establishing Mc2-r as a direct target of Pbx1-dependent action. Although the proximity of binding sites for the two transcription factors implies direct protein-protein interaction of Pbx1 and Sf-1, immunoprecipitation provides no evidence for direct physical binding of the two transcription factors under the chosen experimental conditions. In addition, promoter experiments using a Mc2-r construct with site-directed mutated Sf-1-binding sites argue for Pbx1-induced promoter activation independent from Sf-1. Conversely, an artificial promoter construct consisting of multiple Sf-1-binding sites is not activated by Pbx1. Taken together, these findings suggest a parallel albeit independent promoter activation of the Mc2-r promoter by Pbx1 and Sf-1. However, Pbx1 has been demonstrated to penetrate inactive chromatin structures to facilitate the access of other transcription factors to appropriate promoter regions (3). In this regard, we cannot exclude the possibility that *in vivo* Pbx1 could also facilitate Sf-1 binding to DNA, thus boosting its transcriptional activity.

Because Sf-1 expression in adrenals from Pbx1-deficient embryos has been reported to be reduced (15), these findings indicate a Pbx1-dependent transcriptional activation of Sf-1 and would place Pbx1 before Sf-1 in the temporal expression of transcription factors during urogenital development. In fact, in a recently published paper, Zubair and co-workers (16) provide ample evidence for a Pbx1-dependent initiation of Sf-1 transcription during early adrenal development that is further maintained by a positive auto-feedback loop by Sf-1 itself at later developmental stages. These findings indicate that Pbx1-dependent transcriptional activation of Sf-1 is dependent on the physiological and cellular context. In fact, as shown herein, Sf-1 expression levels in adrenals from Pbx1 haploinsufficient animals are not diminished in comparison with wild-type controls, and overexpression of Pbx1 in adrenocortical Y1 cells does not affect endogenous Sf-1 expression. Although we cannot exclude the possibility that one remaining allele of Pbx1 is sufficient to drive full expression of Sf-1 in adrenals of $Pbx1^{+/-}$ animals, it is also possible that transcriptional regulation of Sf-1 in the adult organism differs from that during early organogenesis.

Conversely, we present evidence suggesting that Sf-1 induces up-regulation of Pbx1 transcription. First, up-regulation of endogenous Pbx1 can be induced by overexpression of Sf-1 in adrenocortical Y1 cells. Second, sequence analysis of the Pbx1 promoter reveals the presence of four Sf-1-binding sites containing the consensus sequence CAAGG (positions −11 to −15 and −2465 to −2454) and AGGTCA (po-

Downloaded from endo.endojournals.org by on February 21, 2008

sitions −2465 to −2460 and −2312 to −2307) (32). Third, cloning of the 5′ region of the Pbx1 gene and subsequent luciferase experiments demonstrate promoter activation of the Pbx1 promoter fragment by Sf-1 in a dose-dependent manner. Fourth, adrenal Pbx1 levels are down-regulated in Sf-1 haploinsufficient animals. Although differences in the spatiotemporal expression patterns between Pbx1 and Sf-1 with organ-restricted expression for Sf-1 and with ubiquitous and early expression for Pbx1 clearly indicate that Sf-1 is not mandatory for Pbx1 expression *in vivo*, down-regulation of Pbx1 in Sf-$1^{+/-}$ mice suggests modulation of Pbx1 transcription by Sf-1 most likely in concert with other transcription factors. In keeping with this notion, as we can demonstrate in promoter studies (data not shown), WT-1 is also able to induce transcriptional activation of Pbx1, which in itself might be of functional significance for urogenital organogenesis. In addition, overexpression of Pbx1 itself results in up-regulation of its own promoter, forming a positive feedback loop system that might contribute to a more stable expression of Pbx1 in its target cells. Overall, it is tempting to speculate that the adrenal phenotype in homozygous and heterozygous Sf-1 knockout animals might be mediated in part by effects of Pbx1 down-regulation resulting in the phenotypical similarities between Sf-1- and Pbx1-deficient mouse models.

In conclusion, we demonstrate that Pbx1, in addition to its involvement in urogenital development and adrenocortical cell commitment, is also required for the growth maintenance of the adult adrenal gland. Furthermore, we present data suggesting that the growth defects observed in Pbx1 haploinsufficient mice are mainly caused by a defect in adrenal cell proliferation under baseline and stimulated conditions. In accordance with the overall similarity in the phenotypes of mouse models with haploinsufficiency for Pbx1 and Sf-1, we provide additional evidence for cooperative interaction between the two transcription factors relying on transcriptional regulation of Pbx1 by Sf-1 as well as synergistic up-regulation of mutual target genes such as the Mc2-r.

Acknowledgments

We are indebted to Igor Shapiro and Timm Stahl (both at Albert-Ludwigs University, Freiburg, Germany) for excellent technical assistance, Dr. Keith Parker (University of Texas Southwestern Medical Center, Dallas, TX), Dr. Oliver Zwermann (Ludwig-Maximilians University, Munich, Germany), Dr. Ken Morohashi (NIBB, Japan) and Dr. Yacob Weinstein (Ben Gurion University of the Negev, Beer Sheva, Israel) for the generous gift of the artificial Sf-1 promoter and Sf-1 expression vector, Mc2-r promoter constructs, Sf-1 antibody and 20αhsd antibody, respectively.

Received May 19, 2006. Accepted October 23, 2006.

Address all correspondence and requests for reprints to: Felix Beuschlein, M.D., Division of Endocrine Research, Department of Medicine Innenstadt, University Hospital Munich, Ziemssenstrasse 1, D-80336 Munich, Germany. E-mail: felix.beuschlein@med.uni-muenchen.de.

This work was supported by a grant from the Landesstiftung Baden-Würtemberg (P-LS-ASN/5) to F.B., a grant from the Deutsche Forschungsgemeinschaft (DFG Schee351/3.1) to J.S., and a National Institutes of Health grant (NIH DK054480) to N.R.S.

Disclosure Statement: The authors have nothing to disclose.

References

1. **Mann RS, Chan SK** 1996 Extra specificity from extradenticle: the partnership between HOX and PBX/EXD homeodomain proteins. Trends Genet 12:258–262
2. **Peltenburg LT, Murre C** 1997 Specific residues in the Pbx homeodomain differentially modulate the DNA-binding activity of Hox and Engrailed proteins. Development 124:1089–1098
3. **Berkes CA, Bergstrom DA, Penn BH, Seaver KJ, Knoepfler PS, Tapscott SJ** 2004 Pbx marks genes for activation by MyoD indicating a role for a homeodomain protein in establishing myogenic potential. Mol Cell 14:465–477
4. **Chang CP, Jacobs Y, Nakamura T, Jenkins NA, Copeland NG, Cleary ML** 1997 Meis proteins are major in vivo DNA binding partners for wild-type but not chimeric Pbx proteins. Mol Cell Biol 17:5679–5687
5. **Goudet G, Delhalle S, Biemar F, Martial JA, Peers B** 1999 Functional and cooperative interactions between the homeodomain PDX1, Pbx, and Prep1 factors on the somatostatin promoter. J Biol Chem 274:4067–4073
6. **Knoepfler PS, Bergstrom DA, Uetsuki T, Dac-Korytko I, Sun YH, Wright WE, Tapscott SJ, Kamps MP** 1999 A conserved motif N-terminal to the DNA-binding domains of myogenic bHLH transcription factors mediates cooperative DNA binding with pbx-Meis1/Prep1. Nucleic Acids Res 27:3752–3761
7. **DiMartino JF, Selleri L, Traver D, Firpo MT, Rhee J, Warnke R, O'Gorman S, Weissman IL, Cleary ML** 2001 The Hox cofactor and proto-oncogene Pbx1 is required for maintenance of definitive hematopoiesis in the fetal liver. Blood 98:618–626
8. **Kim SK, Selleri L, Lee JS, Zhang AY, Gu X, Jacobs Y, Cleary ML** 2002 Pbx1 inactivation disrupts pancreas development and in Ipf1-deficient mice promotes diabetes mellitus. Nat Genet 30:430–435
9. **Schnabel CA, Godin RE, Cleary ML** 2003 Pbx1 regulates nephrogenesis and ureteric branching in the developing kidney. Dev Biol 254:262–276
10. **Selleri L, Depew MJ, Jacobs Y, Chanda SK, Tsang KY, Cheah KS, Rubenstein JL, O'Gorman S, Cleary ML** 2001 Requirement for Pbx1 in skeletal patterning and programming chondrocyte proliferation and differentiation. Development 128:3543–3557
11. **Lawrence HJ, Helgason CD, Sauvageau G, Fong S, Izon DJ, Humphries RK, Largman C** 1997 Mice bearing a targeted interruption of the homeobox gene HOXA9 have defects in myeloid, erythroid, and lymphoid hematopoiesis. Blood 89:1922–1930
12. **Carpenter EM, Goddard JM, Davis AP, Nguyen TP, Capecchi MR** 1997 Targeted disruption of Hoxd-10 affects mouse hindlimb development. Development 124:4505–4514
13. **Condie BG, Capecchi MR** 1993 Mice homozygous for a targeted disruption of Hoxd-3 (Hox-4.1) exhibit anterior transformations of the first and second cervical vertebrae, the atlas and the axis. Development 119:579–595
14. **Kagawa N, Ogo A, Takahashi Y, Iwamatsu A, Waterman MR** 1994 A cAMP-regulatory sequence (CRS1) of CYP17 is a cellular target for the homeodomain protein Pbx1. J Biol Chem 269:18716–18719
15. **Schnabel CA, Selleri L, Cleary ML** 2003 Pbx1 is essential for adrenal development and urogenital differentiation. Genesis 37:123–130
16. **Zubair M, Ishihara S, Oka S, Okumura K, Morohashi K** 2006 Two-step regulation of Ad4BP/SF-1 gene transcription during fetal adrenal development: initiation by a Hox-Pbx1-Prep1 complex and maintenance via autoregulation by Ad4BP/SF-1. Mol Cell Biol 26:4111–4121
17. **Chui D, Oh-Eda M, Liao YF, Panneerselvam K, Lal A, Marek KW, Freeze HH, Moremen KW, Fukuda MN, Marth JD** 1997 α-Mannosidase-II deficiency results in dyserythropoiesis and unveils an alternate pathway in oligosaccharide biosynthesis. Cell 90:157–167
18. **Luo X, Ikeda Y, Parker KL** 1994 A cell-specific nuclear receptor is essential for adrenal and gonadal development and sexual differentiation. Cell 77:481–490
19. **Babu PS, Bavers DL, Beuschlein F, Shah S, Jeffs B, Jameson JL, Hammer GD** 2002 Interaction between Dax-1 and steroidogenic factor-1 *in vivo*: increased adrenal responsiveness to ACTH in the absence of Dax-1. Endocrinology 143:665–673
20. **Beuschlein F, Mutch C, Bavers DL, Ulrich-Lai YM, Engeland WC, Keegan C, Hammer GD** 2002 Steroidogenic factor-1 is essential for compensatory adrenal growth following unilateral adrenalectomy. Endocrinology 143:3122–3135
21. **Bicknell AB, Lomthaisong K, Woods RJ, Hutchinson EG, Bennett HP, Gladwell RT, Lowry PJ** 2001 Characterization of a serine protease that cleaves pro-γ-melanotropin at the adrenal to stimulate growth. Cell 105:903–912
22. **Chen WY, Juan LJ, Chung BC** 2005 SF-1 (nuclear receptor 5A1) activity is activated by cyclic AMP via p300-mediated recruitment to active foci, acetylation, and increased DNA binding. Mol Cell Biol 25:10442–10453
23. **Zwermann O, Beuschlein F, Lalli E, Klink A, Sassone-Corsi P, Reincke M** 2005 Clinical and molecular evidence for DAX-1 inhibition of steroidogenic factor-1-dependent ACTH receptor gene expression. Eur J Endocrinol 152: 769–776
24. **Sanchez M, Jennings PA, Murre C** 1997 Conformational changes induced in Hoxb-8/Pbx-1 heterodimers in solution and upon interaction with specific DNA. Mol Cell Biol 17:5369–5376
25. **Schnabel CA, Jacobs Y, Cleary ML** 2000 HoxA9-mediated immortalization of myeloid progenitors requires functional interactions with TALE cofactors Pbx and Meis. Oncogene 19:608–616
26. **Pan L, Xie Y, Black TA, Jones CA, Pruitt SC, Gross KW** 2001 An Abd-B class

Downloaded from endo.endojournals.org by on February 21, 2008

HOX.PBX recognition sequence is required for expression from the mouse Ren-1c gene. J Biol Chem 276:32489–32494
27. **Engeland WC, Dallman MF** 1976 Neural mediation of compensatory adrenal growth. Endocrinology 99:1659–1662
28. **Naville D, Penhoat A, Durand P, Begeot M** 1999 Three steroidogenic factor-1 binding elements are required for constitutive and cAMP-regulated expression of the human adrenocorticotropin receptor gene. Biochem Biophys Res Commun 255:28–33
29. **Berthelsen J, Zappavigna V, Mavilio F, Blasi F** 1998 Prep1, a novel functional partner of Pbx proteins. Embo J 17:1423–1433
30. **Ferretti E, Cambronero F, Tumpel S, Longobardi E, Wiedemann LM, Blasi F, Krumlauf R** 2005 Hoxb1 enhancer and control of rhombomere 4 expression: complex interplay between PREP1-PBX1-HOXB1 binding sites. Mol Cell Biol 25:8541–8552
31. **McWhirter JR, Goulding M, Weiner JA, Chun J, Murre C** 1997 A novel fibroblast growth factor gene expressed in the developing nervous system is a downstream target of the chimeric homeodomain oncoprotein E2A-Pbx1. Development 124:3221–3232
32. **Morohashi K, Honda S, Inomata Y, Handa H, Omura T** 1992 A common trans-acting factor, Ad4-binding protein, to the promoters of steroidogenic P-450s. J Biol Chem 267:17913–17919
33. **Bland ML, Jamieson CA, Akana SF, Bornstein SR, Eisenhofer G, Dallman MF, Ingraham HA** 2000 Haploinsufficiency of steroidogenic factor-1 in mice disrupts adrenal development leading to an impaired stress response. Proc Natl Acad Sci USA 97:14488–14493
34. **Bland ML, Fowkes RC, Ingraham HA** 2004 Differential requirement for steroidogenic factor-1 gene dosage in adrenal development versus endocrine function. Mol Endocrinol 18:941–952
35. **Spencer SJ, Mesiano S, Lee JY, Jaffe RB** 1999 Proliferation and apoptosis in the human adrenal cortex during the fetal and perinatal periods: implications for growth and remodeling. J Clin Endocrinol Metab 84:1110–1115
36. **Zajicek G, Ariel I, Arber N** 1986 The streaming adrenal cortex: direct evidence of centripetal migration of adrenocytes by estimation of cell turnover rate. J Endocrinol 111:477–482
37. **Mesiano S, Jaffe RB** 1997 Role of growth factors in the developmental regulation of the human fetal adrenal cortex. Steroids 62:62–72
38. **Giordano TJ, Thomas DG, Kuick R, Lizyness M, Misek DE, Smith AL, Sanders D, Aljundi RT, Gauger PG, Thompson NW, Taylor JM, Hanash SM** 2003 Distinct transcriptional profiles of adrenocortical tumors uncovered by DNA microarray analysis. Am J Pathol 162:521–531
39. **Hoeflich A, Weber MM, Fisch T, Nedbal S, Fottner C, Elmlinger MW, Wanke R, Wolf E** 2002 Insulin-like growth factor binding protein 2 (IGFBP-2) separates hypertrophic and hyperplastic effects of growth hormone (GH)/IGF-I excess on adrenocortical cells in vivo. FASEB J 16:1721–1731
40. **Yaswen L, Diehl N, Brennan MB, Hochgeschwender U** 1999 Obesity in the mouse model of pro-opiomelanocortin deficiency responds to peripheral melanocortin. Nat Med 5:1066–1070
41. **Mountjoy KG, Robbins LS, Mortrud MT, Cone RD** 1992 The cloning of a family of genes that encode the melanocortin receptors. Science 257:1248–12451

***Endocrinology* is published monthly by The Endocrine Society (http://www.endo-society.org), the foremost professional society serving the endocrine community.**

Downloaded from endo.endojournals.org by on February 21, 2008